Journal of Materials & Manufacturing, Vol.107, Section 5 980082

Using Neural Network for Springback Minimization in a Channel Forming Process

R. Ruffini
Dipartimento di Meccanica, University of Ancona, 60131 Ancona, Italy

J. Cao
Department of Mechanical Engineering, Northwestern University, Evanston, Ill, 60208-3111

ABSTRACT

Springback, the geometric difference between the loaded and unloaded configurations, is affected by many factors, such as material properties, sheet thickness, lubrication conditions, tooling geometry and processing parameters. It is extremely difficult to develop an analytical model for springback control including all these factors. The proposed neural network model is an attempt to deal with such a complicated non-linear system in a predictive way. For demonstration, an aluminum channel forming process is considered in this work. Our previous research [1] has shown that a variable binder force history during the forming operation can reduce the springback amount significantly while maintaining a relatively low maximum strain if an initial low binder force was used followed by a higher binder force. However, when and how much of the increase is depends on the forming conditions of the current process. Here, several numerical simulations using Finite Element Method (FEM) were performed to obtain the teaching data required for training the neural network by means of the back-propagation algorithm. In the predictive mode, different process inputs from the ones used in the previous stage were considered. For each case, the displacement where binder force increases and the level of the high binder force were predicted by the learned neural network and were numerically tested. Consistent low springback angle (< 0.5°) and moderate stretching amount (< 16%) were obtained even in the cases where the process parameters were varied as much as ±25% on friction coefficient and sheet thickness or ±10% on material's mechanical properties. The neural network can be easily implemented in the experiments and/or in real production to resolve the uncertainty of springback amount due to the variations in material properties and friction conditions.

INTRODUCTION

One of the largest challenges in manufacturing is the consistency of final products. Two basic approaches have been investigated to achieve this goal. One is to use intelligent assembly methodologies to select a suitable set of parts to be assembled, that is, taking advantage of tolerance stack up. However, to our knowledge, no fundamental theory on how to efficiently select the parts has been developed and applied to various manufacturing processes. The other approach aims at each individual manufacturing process module, for example, sheet metal forming process, which is the approach and the focus of this work.

As known, during unloading (tooling retreat) in the forming process, the elastic component of the stress generated during the deformation is released leading to a partial return of the deformed part toward the initial configuration. This is so-called 'Springback', which has been intensively studied in many recent proceedings of NUMISHEET and SAE conferences. To minimize the geometrical errors in the final shape, the reduction and the consistency of the springback are the two key issues. Springback can be reduced by a proper tooling design (die design, binder design, etc.) or by controlling the magnitude and the history of the plastic stretch imposed to the sheet by a proper binder force trajectory (process control). Karafillis and Boyce [2,3] proposed a method, "SpringForward", for tool and binder design to obtain the desired part shape. Using finite element analysis of a forming process, the amount of springback and its associated section bending moment can be calculated and fedback to a tooling design algorithm, which provides the new tooling shape compensating the springback. The design process is repeated until reaching the desired springback amount. The "SpringForward" method provides a powerful tool for designing the tooling taking the amount of potential springback into account. The tooling geometry is often not the same as the desired part geometry. However, "SpringForward" is not designed to and therefore, not able to deal with the variations in the processes. In the aspect of the process design, Ayres [4] developed a

'passive' two-step SHAPESET process and Sunseri, Cao et al. [1] proposed a strategy to actively control the binder force during the forming operation. In both works, springback was reduced by having two levels of binder force in the forming process. Ayres [4] achieved the goal by having two different die sets and Sunseri et al [1] utilised an active binder force controller. Using a VBF trajectory, the springback amount was less than 1.14° [1]. Furthermore, in order to maintain stable performances in springback control at the presence of variations in lubrication conditions, a real-time closed-loop control of the binder force was implemented to achieve the same punch force history [1]. The approach was able to obtain the consistent springback amount when friction coefficient was varied from 0.25 to 0.10. However, the effectiveness of the proposed approach under large scattering in material properties and sheet thickness was not discussed.

An alternative approach for obtaining consistent springback amount could be the development of an artificial neural network model system capable of dealing with such arbitrary non-linear systems. Artificial neural networks have been studied for many years in the hope of achieving human-like performances in solving problems that are generally ill defined and require a great amount of processing. Human brains accomplish this data processing by utilizing massive parallelism, with millions of neurons working together to solve complicate problems. Similarly, artificial neural network models consist of many computational elements operating in parallel connected by links with variable weights that are typically adapted during the learning process. Development of detailed mathematical models began in the 1960s with the works of Rosenblatt [5] and Widrow [6] in the years following these discoveries, many new techniques have been developed in the field of neural networks and the discipline is growing rapidly. More recent applications regard vehicular control simulation [7], speech generation [8], speech recognition [9] and expert systems [10].

In recent years, applications of artificial neural in sheet metal forming process control have been also proposed. For example, an attempt to apply a neural network control scheme for springback reduction in a 60° V-punch air bending process of an aluminium alloy was made, among other authors [11-12], by Forcellese et al. [13]. Five parameters describing the measured punch force-displacement curve were utilized as input data during the neural network training; additional inputs included the sheet thickness and the bend angle after unloading. The system was trained on several sets of experimental data. In the predictive mode, the target angle, the off-line measured sheet thickness and the "in-process" estimated parameters were given as inputs to the trained neural network to determine the appropriate punch stroke for the desired bend angle. The work had one process parameter and required the offline measurement of sheet thickness, which adds additional cost to manufacturing.

In this paper, the objective of our work is to resolve the problem of springback reduction for a more complicated sheet metal forming process using a neural network based control system. FEM simulations of a channel forming process of sheets from an aluminium alloy are used for demonstration. A step function as proposed in Sunseri et al [1] is used as the binder force history. The effects of lubrication conditions, sheet thickness and material properties on springback are considered. Since all these factors affect the punch force-displacement curve, 8 parameters characterizing such a curve are considered as inputs to learn the neural network. The output pattern is constituted by the punch stroke corresponding to the increase in the binder force and by the level of the high binder force, the lower binder force is set constant. Despite of large variations on material parameters and friction conditions (±10% and ±25%, respectively), excellent results were obtained -- a consistent springback angle of less than 0.3°.

Although the methodology is verified by means of the numerical simulation, the method can been easily implemented in experiments and/or on manufacturing floor as well. The requirements of the hardware are an extremely low powered CPU, the ability to measure the punch force-displacement data in "real–time" and the ability setting binder force during the press cycle. Many new presses in stamping plants have the above capacity. The optimal binder force trajectory for controlling and minimizing the springback will then be adjusted based on the current manufacturing conditions. This design indeed provides a very robust control system at a very low cost.

CHANNEL FORMING PROCESS AND ITS FINITE ELEMENT MODEL

As is generally known, springback is due to the uneven distribution of stress states in the loading configuration. This fact can be easily demonstrated in a channel forming operation where the entire punch stroke is 19.2 mm (Fig. 1). Figure 2 shows a quarter model of the channel forming in Finite Element Analysis using a commercial package (ABAQUS 1997). The binder, the die and the punch were modelled as three separate rigid surfaces and each surface was modelled using four-node interface elements (ABAQUS type IRS4) and taken to be frictional. A Coulomb friction law was assumed. With proper symmetric conditions applied on A-A and B-B section, the entire blank of 220mm x 46mm was modelled by 40 x 4 four-node shell elements with reduced integration (ABAQUS type S4R). The material was modelled to be isotropic elastic-plastic following the Mises yield criterion and isotropic strain hardening. The elastic properties were the tensile modulus E=70GPa and Poisson ratio ν=0.3. The plastic behavior of the material is modelled using a power law relation ($\sigma=K\varepsilon^n$) with a material strength coefficient *K* of 528 MPa and a strain hardening component *n* of 0.265. The forces reported here are of a quarter model.

Fig. 1 Geometry of the channel forming.

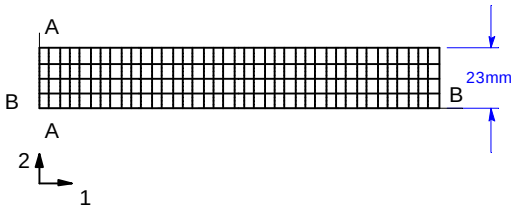

Fig. 2a Finite element mesh of the blank.

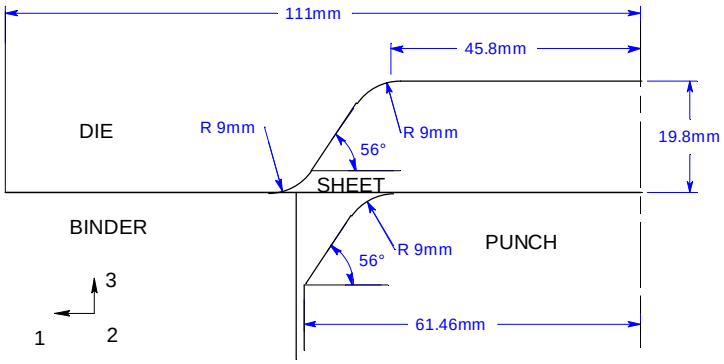

Fig. 2b Finite element model of the channel forming.

THE NEURAL NETWORK AND THE BACK-PROPAGATION ALGORITHM

Multi-layer neural networks are fed-forward nets with one or more layers of nodes between the input and output ones (hidden layers). In a fully connected layered network, each neuron receives inputs from all the elements in the preceding layer; no connection exists between neurons belonging to the same layer.

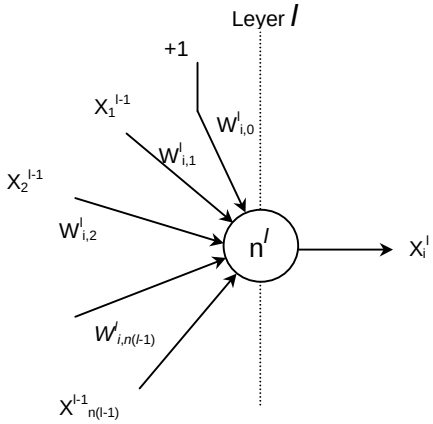

Fig. 3 Model of artificial neuron

At ada  input vector). The output

$$X_i^l = f(W_{i,0}^l + \sum_{j=1}^{n(l-1)} W^l{}_{i,j} \times X_j^{l-1}) \qquad (1)$$

where $n(l\text{-}1)$ is the number of elements in the layer l-1, f is the activation function, and $W^l_{i,j}$ is the weight associated with the connection between the neuron i in the layer l and the neuron j in the layer l-1 whose output is X_j^{l-1}. Usually, the input $W^l_{i,0}$ is a constant and equal to 1 so that the corresponding weight (offset or Bias) shifts the activation function along the abscises axis.

During learning, Q sets of input and output data (Q input-output patterns) are provided to the neural network. An iterative algorithm adjusts the weights so that the responses (y) generated at output nodes (Eqn. 1) according to the input patterns will be as close as possible to their respective desired responses (d). Considering a neural network with N_0 outputs, the Mean Square Error function (MSE) is to be minimized:

$$\mathrm{MSE} = \frac{1}{Q \times N_0} \times \sum_{m=1}^{Q} \sum_{n=1}^{N_0} (d_n[m] - y_n[m])^2 \qquad (2)$$

The back-propagation algorithm [14, 15] is most widely used to minimize MSE. It is based on the current pattern error estimation and works with one pattern at a time. For each neuron, the gradient of the current MSE function is measured and the weight vector is altered in the direction corresponding to the negative measured gradient following

$$\mathbf{W}_{k+1} = \mathbf{W}_k + \eta(-\nabla_k) \qquad (3)$$

where η, the learning rate, is the parameter controlling the stability and rate of convergence and ∇_k is the gradient of the local squared error corresponding to $\boldsymbol{W} = \boldsymbol{W}_k$. Details can be found in [16]. The effects of errors on each output are swept backward through the network to associate a "square error derivative" δ_i^l to each element i somewhere in layer l. It can be shown that each square error derivative for neurons in the output layer is computed by multiplying the output error associated with that element by the derivative of the associated activation function. For the other layers, the square error derivative for a given neuron is obtained by multiplying each derivative δ_i^{l+1} associated to each neuron in the layer immediately downstream by the weight that connects it to the given neuron. These weighted square-error derivatives are then added together and multiplied by the derivative of the given element's activation function calculated at its operation point. This process of backpropagation is repeated until that a square error

derivative is computed for each element in the network.

Finally, the relationship between the gradient and the square error derivative is:

$$\nabla_k = -2\delta_k \boldsymbol{X}_k \qquad (4)$$

From equations (3) and (4) it follows:

$$\mathbf{W}_{k+1} = \mathbf{W}_k + 2\eta\delta_k X_k \qquad (5)$$

A back-propagation iteration is applying Eqn. 5 to each neuron of the network. The process restarts with a new input-output pattern presentation. Once the weights are adjusted, the responses of the trained system can be tested by supplying various input patterns. If the network responds correctly to input patterns that were not included in the training set, it is said that generalisation has taken place. To demonstrate its applicability in real problems, Cybenko [17] has shown that given sufficient number of hidden elements, feedforward networks with two hidden layers with sigmoidal activation function can implement any continuous input-output mapping to arbitrary accuracy. Consequently, it is appropriate to regard neural networks as a control model capable of dealing with non-linear systems. Furthermore, once the generalization performance has been verified, the training set can be continuously updated improving the neural network modeling capability.

PROCESS ANALYSIS

In this section, constant binder force (CBF) and variable binder force (VBF) will be studied to demonstrate the advantage of VBF and to explore the feasibility of using punch force history as the signature of the forming conditions.

CONSTANT BINDER FORCE

The conventional forming process utilizes the same binder force throughout the drawing process. Numerical FEM simulations were performed in order to examine the effect of a constant binder force (CBF) upon springback after unloading. The stamping process of a workpiece of 1 mm with friction coefficient μ =0.16 is considered for demonstration. Simulations were performed for cases of CBF varying from 4 kN to 36 kN. The unloaded and desired configurations for the two extreme cases of CBF are shown in Fig.4, while the corresponding values of the springback angle θ are depicted in Fig.5.

It can be observed that very large deviation in shape occurs with the lower binder force case and how it is gradually reduced with the increasing of the restraining force. In the low binder force conditions, due to the substantially bending nature of the process, one side of the sheet is in compression and the other side is in tension; consequently, a large internal bending moment is generated leading to a large amount of springback after unloading. Conversely, with increasing the plastic stretch induced in the sheet, the gradient of the stress distribution throughout the thickness is gradually reduced leading to a decreasing in springback. However the decrease in the internal bending moment is achieved with a large increase of the maximum principal strain $\varepsilon_{11(max)}$ as shown in Fig.6. In order to obtain acceptable amount of springback ($\theta < 0.5°$) under CBF conditions, the maximum level of ε_{11} must increase approaching the limit of material failure. In fact, the Forming Limit Diagram for this material shows a failure strain of 19 % [18] in plane strain.

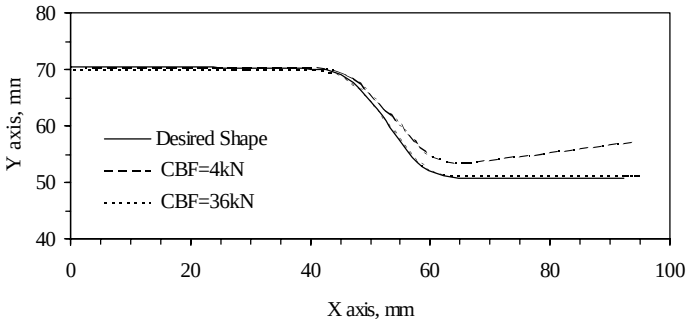

Fig.4 Shape of the formed part and final configurations;

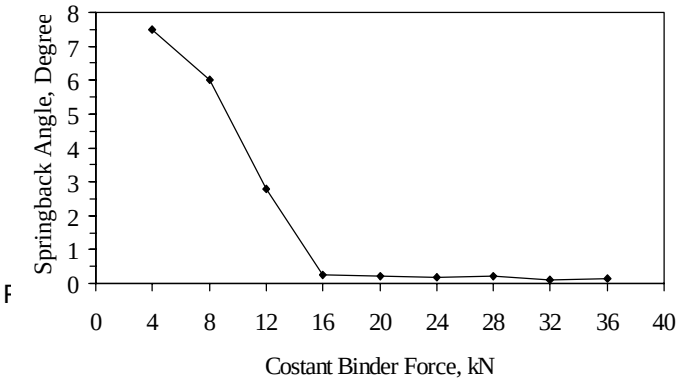

Fig.5 Springback angle: constant binder force, t = 1 mm, μ = 0.16

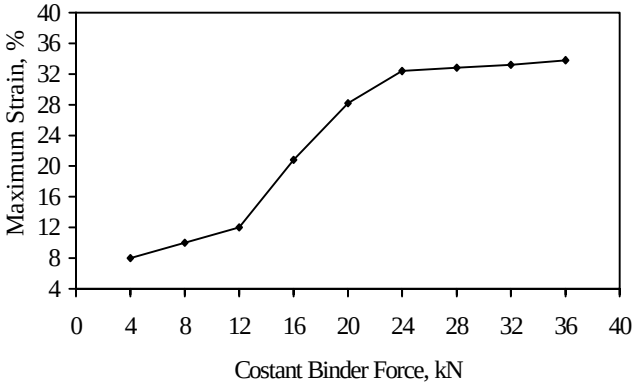

Fig. 6 Maximum stretch as a function of CBF, t = 1 mm, μ = 0.16

VARIABLE BINDER FORCE

As proposed by Sunseri, Cao et. al. [4], Variable Binder Force (VBF) histories were considered in order to reduce the springback angle without producing too large deformations in the formed part. An initial low binder force is used to allow the metal to flow easily into the die cavity to obtain a preliminary shape. Springback is severe at the end of this step due to the essentially bending working state that characterises the deformation. At the later stage of punch stroke, the binder force is instantaneously increased to a higher value in order to introduce a larger amount of stretching with respect to the previous forming stage. By selecting the punch travel where the high binder force is applied and the level of the higher binder force, springback minimization can be obtained and associated to a remarkable reduction in the maximum principal strain incurred in the formed part. For the process parameters considered in this section, simulations have shown that a very good result is obtained for the case in which the load is increased from 4kN to 13 kN at the punch stroke of 75 % of the total stroke. The springback angle is θ = 0.31° and $\varepsilon_{11(max)}$ = 11.78 %. Figure 7 shows both the desired and the unloaded shapes for this case; the step function that describes the binder force trajectory is shown in Fig.8. The corresponding Punch force-displacement curve is depicted in Fig. 9 together with the punch force trajectories of two extreme CBF cases.

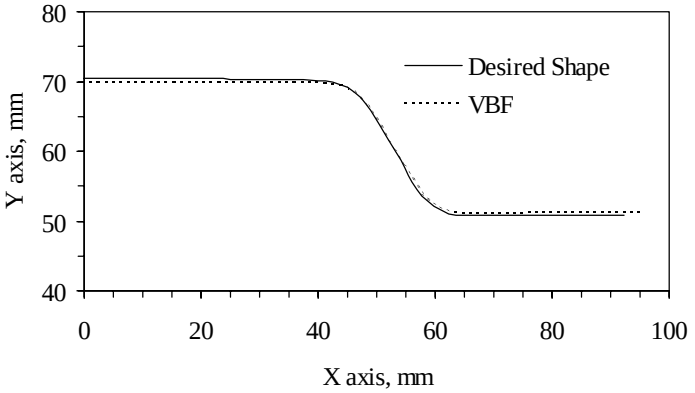

Fig. 7 Part shape after springback for the variable binder force case.

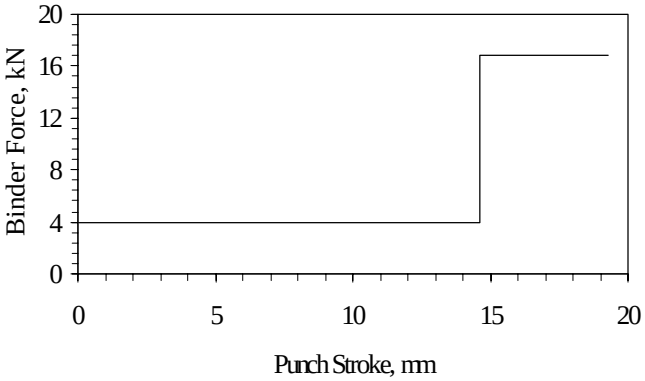

Fig. 8 Variable binder force history

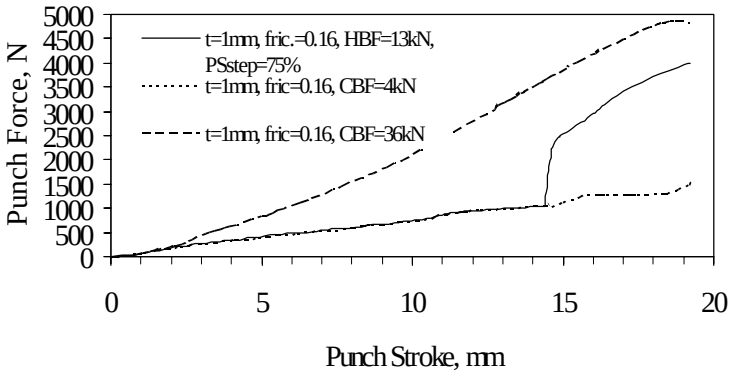

Fig. 9 Punch force history for the variable binder force case

In any case, the selections of both the timing for applying the additional stretch and the level of the high binder force are critical aspects in order to obtain good results in terms of springback reduction and integrity of the final product.

SPRINGBACK REDUCTION UNDER SCATTERING IN FRICTION CONDITIONS AND SHEET THICKNESS

The neural network capability in springback minimization for the forming process with variations in lubrication conditions and in sheet thickness is investigated in this section. The material characteristics are kept the same as described in section 2.

TRAINING OF THE NETWORK

12 various sets of friction coefficient and thickness are used as the training cases. Friction coefficient was varied from 0.12 to 0.2 with an increment of 0.02 and sheet thickness was varied from 0.8 mm to 1.2 mm with an increment of 0.2mm. For each combination of friction coefficient μ and sheet thickness, 10 different step functions of the binder force history were tested in the FEM simulations with an initial low binder force of 4kN. In order to decrease the probability of failure and improve the integrity of the formed part, results from simulations leading to a maximum principal strain ε_{11} greater than 16% were not considered. Finally, the simulation characterized by the lower springback angle was chosen as the teaching set for the neural network training as shown in Table 1.

Columns 3 and 4 show respectively the level of the High Binder Force (HBF) and the punch position (PS_{step}) at which the binder force is instantaneously increased to the higher value. The springback angle and the maximum strain achieved at the end of the process are reported in columns 5 and 6. Notice that those shown above are not guaranteed to be the “best” possible solutions; they rather represent a selected set of possible ones for springback reduction to an acceptable level. For each sheet thickness, it can be observed that the level of HBF decreases as the friction coefficient increases. It’s well known that the reduction in the level of friction reduces the restraining force imparted to the

sheet thereby reducing stretching and increasing springback; consequently a greater binder force is required for springback minimization. Similarly, it can be also seen that considering the same friction coefficient value, a higher restraining force is associated with an thicker sheet; this can be explained considering that more stretching is required for the gradient reduction of the stress distribution throughout the thickness of the workpiece in bending. A similar monotonic behaviour can not be observed in the position of the increase, which scatters in a very random manner; this is the principal reason why a neural network model is utilized to model the relationship between binder force trajectories and process parameters.

Thickness (mm)	Fric. Coeff	HBF KN	PS_{step},% tot. stroke.	θ, (°)	$\varepsilon_{11(max)}$ (%)
0.8	0.12	18	75	0.12	11.76
"	0.14	15	74	0.053	12.61
"	0.16	13	82	0.015	9.82
"	0.20	9	80	0.004	10.74
1	0.12	20	70	0.18	13.59
"	0.14	16	68	0.25	12.97
"	0.16	13	75	0.31	11.52
"	0.20	10	72	0.24	11.78
1.2	0.12	24	71	0.16	13.34
"	0.14	21	68	0.176	14.81
"	0.16	16	74	0.3	13.54
"	0.20	13	71	0.22	14.64

Table 1 – Set of FEM simulations for training neural network

Figures 10 describe the punch force-displacement curves obtained by the numerical simulations for the cases shown in Table 1. It can be seen how variations in process parameters lead to remarkable differences in the behaviour of the punch force history.

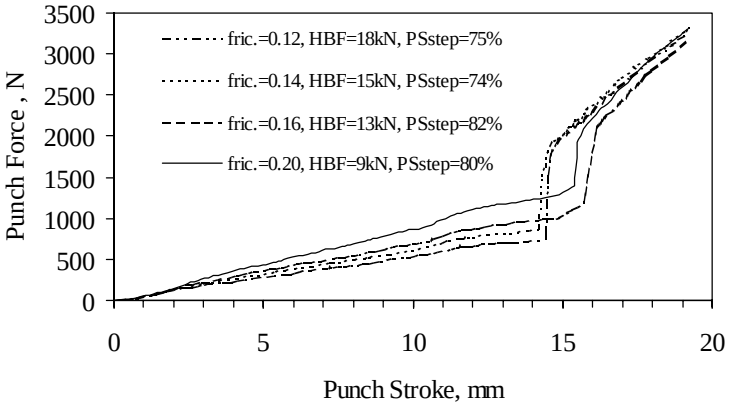

Fig. 10(a) Punch force-displacement curves, numerical results - Thickness = 0.8 mm

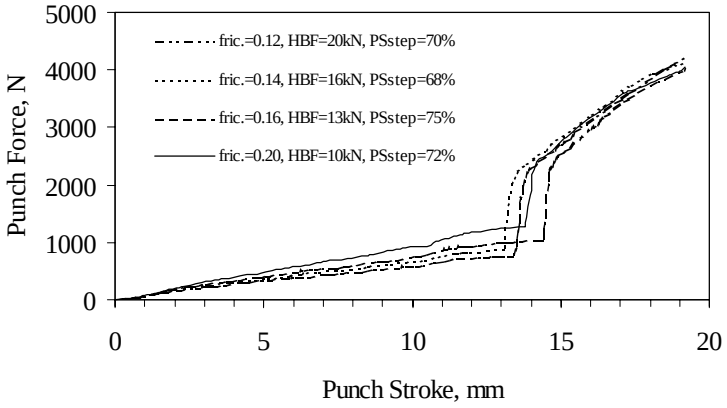

Fig. 10(b) Punch force-displacement curves, numerical results - t = 1 mm

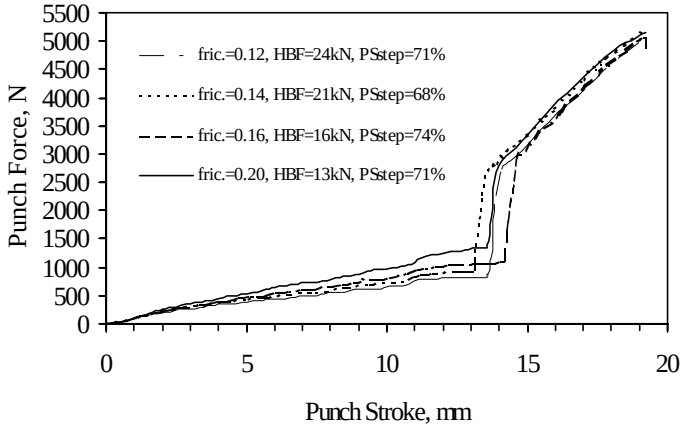

Fig. 10(c) Punch force-displacement curves, numerical results - t= 1.2 mm

Furthermore, material properties affect the punch force-stroke data as well. For this reason, the mechanical behaviour of the sheet during deformation is described in this work by the coefficients obtained by the least square polynomial fitting of the curves shown in figures 10, such parameters are estimated on the "real-time" punch force-displacement data. Stelson [20-22] proposed methods for the mechanical characterization of the sheet based on the punch-force displacement data in different metal forming processes. However, since restrictive hypotheses on both the deformation and geometrical modelling were made, such models did not provide results completely error-free. In this work, no simplifying assumptions on the mechanical modelling of the sheet are used. Moreover, the negative errors due to the mathematical manipulation of numerical data are avoided. The force displacement curves were divided in two regions: *Region A*, where the punch strokes less than 1.5 mm. A 4^{th} order polynomial function was used for the curve fitting analysis. *Region B*, where the punch strokes between 3 mm and 10 mm. A polynomial order equal to 3 was considered. Figure 11 shows all the 12 punch force histories where the punch displacements are less than 10 mm.

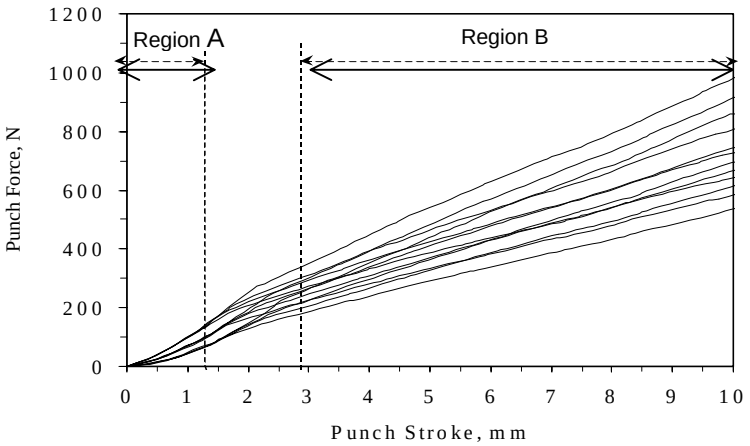

Fig.11 Punch forces vs punch displacement before 10mm for cases in Table 1

Notice that, in Region A, distinguishing differences exist among various thickness and no significant qualitative differences exist among the same sheet thickness. However discrepancies are evident in region B. Data corresponding to displacements from 1.5 mm up to 3 mm were neglected because they were referred to a transition zone between region A and region B. Furthermore, as it will be explained later in this paper, the curve parameters are to be estimated before the end of the forming process. Consequently, the upper limit of region B results from the trade-off of having enough data for a good curve fitting and of being sufficiently lower than the total punch stroke so that real-time control can be executed. From figures 10, it is evident that qualitative differences between the curves are also present for displacement greater than 10 mm. However, as it will be demonstrated later, the data prior to 10mm is sufficient for the neural network control system.

PREDICTIONS OF THE NEURAL NETWORK

An artificial neural network model was developed for the springback minimization in the channel stamping process investigated in this paper. The network is constituted of one input layer, one hidden layer and two output units; no neurons are present in the input layer and each hidden unit receives all the input signals. The net was trained by initially selecting small random weights and internal offsets and then presenting all training data repeatedly. Weights were adjusted after every trial by the backpropagation algorithm outlined in section 2 until the MSE was reduced to an acceptable small value. Each input pattern was formed by the mechanical behaviour parameters obtained by the curve fitting analysis described earlier. Since all the curves pass through the origin in Fig.11, a polynomial coefficient carried out by the regression analysis of the portion of the curves in region A is always equal to zero. Therefore it was not included in the teaching set and 8 parameters (4 for region A and 4 for region B) were used as input signals. The corresponding punch displacement where binder force increases and the level of the high binder force constituted the output patterns.

There are many numbers of network architectures that could be tested. As a general rule, the number of nodes must be large enough to form a map region that is as complex as is required by a given problem. It must not, however, be so large that the many weights required can not be reliably estimated from the available training data. Furthermore, a trained net is of little utility unless it is accomplished by useful generalization.

Several feed-forward fully connected neural networks were investigated in this work, considering different a) topologies (number of layers, number of nodes), b) learning parameters, c) activation functions, and d) initial random weights. Each net was trained to different levels and, among all, the one characterized by the global lowest generalization error was selected; a network with six hidden units provided the best results in generalization. The following activation function was implemented for the elements in the hidden and output layers:

$$f(x) = 2G - \frac{G}{1 + e^{-\alpha x}} \qquad (6)$$

The α and G coefficients in equations (6) were varied accordingly to the speed of convergence in learning. Table 2 shows the learning rate η and the optimal iteration number utilized for training the network and the MSE value achieved at the end of the learning stage.

Iterations	**Learning rate η**	**10 log(MSE)**
100000	0.01	-75

Table 2 Learning coefficients

After the network was trained, it was utilized to predict the forming parameters for 9 different combinations of sheet thickness and friction coefficient from Table 1. The punch was initially displaced to 10 mm (Fig. 11) in the FEM simulations. All the mechanical behaviour parameters were then calculated by performing a polynomial regression analysis of the force-displacement data obtained from the numerical simulations. Finally, the predicted parameters defining the binder force step function were considered to restart the FEM analysis. The results obtained in the predictive mode are shown in Table 3.

Thick-ness mm	Fric. coeff.	HBF kN	PS_{step}, % tot. stroke	θ (°)	$\varepsilon_{11(max)}$ %
t=0.9	0.13	16	76	0.16	11.59
t=0.9	0.15	15	76	0.12	12.08
t=0.9	0.18	12	75	0.03	13.14
t=1.1	0.13	20	75	0.19	12.16
t=1.1	0.15	16	74	0.22	12.40
t=1.1	0.18	13	75	0.22	12.83
t=1	0.15	15	76	0.16	11.99
t=1.2	0.15	20	71	0.15	14.20

Table 3: Neural network predictions

By comparing results shown in Tables 1 and 3, it can be observed that the maximum springback angles obtained using the neural network predictions is consistently lower than the maximum allowed springback angle ($\theta = 0.5°$). Furthermore, it can be noticed that the springback reduction is obtained with low probability of failure in the formed part. In particular, the maximum level of deformation and springback angles are even lower than the maximum value shown in Table 1, confirming the neural network capability of springback minimization in presence of process uncertainties and variations without reaching critical conditions.

EFFECT OF MATERIAL PROPERTIES ON SPRING-BACK IN THE CHANNEL FORMING PROCESS

In real production, variations in material properties occur frequently even in a same coil. In order to take into account such possibilities, the neural network must be robust with respect to the scattering of yield stress σ_y as well as of the n and K coefficients on springback.

MATERIAL PROPERTIES SCATTERING: YIELD STRESS

Two more verification run were performed considering scattering in yield stress (±10% of the nominal YS); the other material properties, such as elastic modulus, Poisson ratio, strain hardening exponent and strength coefficients, were identical to those presented earlier. The friction coefficient and the sheet thickness were μ = 0.12 and t =0.8 mm, respectively. Again, each FEM analysis was stopped at a punch stroke = 10 mm and the mechanical parameters were estimated on the basis of the punch force-displacement data. Since such coefficients describe how the mechanical behaviour of the workpiece is affected by "all" the process conditions, including material properties, the previous learned neural network was utilized to predict the optimal binder force step function for springback reduction in presence of yield stress variation. The results are shown in Table 4. Notice that extreme good results are obtained using the same network

Thick ness (mm)	Fric. Coeff.	HBF KN	PS_{step} %Tot. stroke	θ (°)	$\varepsilon_{11(max)}$ (%)	σ_y Mpa	K MPa	n
0.8	0.12	17	75	0.145	11.9	126	528	0.265
0.8	0.12	21	81	0.005	10.0	154	528	0.265

Table 4 Neural network predictions in the presence of yield stress scattering

MATERIAL PROPERTIES SCATTERING: STRENGTH COEFFICIENT, HARDENING EXPONENT

Variations in the K and n parameters were also evaluated. Taking advantage of the additional data available from the previous predictions, the neural network was trained again using the same learning parameters utilized in the previous training process (Table 2). 120.000 iterations were necessary to obtain about the same final MSE value achieved previously due to the increased number of training data. The results provided by the FEM simulations using the predicted HBF and PS_{step} values are reported in Table 5.

Thick ness (mm)	Fric. Coeff.	HBF KN	PS_{step} %Tot. stroke	θ (°)	$\varepsilon_{11(max)}$ (%)	σ_y Mpa	K MPa	n
0.8	0.12	18	82	0.21	8.77	140	560	0.29
0.8	0.12	16	76	0.123	10.0	140	500	0.25

Table 5 Neural network predictions in presence of n and K scattering

In all the above cases, excellent results were obtained, confirming once again the effectiveness of neural networks in springback reduction with variations from lubrication, sheet thickness and material property.

SUMMARY

A neural network control system for springback reduction in a channel section stamping process of aluminum was proposed in this paper.

- Influences of variations in both sheet thickness *t* and lubrication conditions μ were examined. Although a monotonic behavior in the level of High Binder Force (HBF) characterizing the teaching data in terms of μ

and *t* individually can be observed, the punch displacement corresponding to the increase in the binder force scatters in a vary random manner. In addition, the effects of μ and *t* are highly coupled. This initiates the investigation of using an artificial neural network control system for the reduction of angular errors.

- The punch force history is identified as the characteristic parameter since it reflects the changes of μ, *t* and material properties. 8 parameters were used to characterize each individual punch force behavior.

- By selecting appropriate VBF histories for the teaching data, the learned neural network was able to predict an optimal binder force trajectory for springback minimization without reaching failure conditions in the formed part. Once the best net morphology was individuated, the learning process was performed very easily and quickly.

- Variation in material properties was considered for a given sheet thickness and friction condition. The relationship between springback and such variations was modeled very well by the neural network, confirming the capability of the proposed approach of dealing with all the process conditions uncertainties considered in this paper.

Although FEM simulations of the stamping process were used, the method can be utilized in real production as well. After the network is learned, the mechanical behavior parameters can be determined in "real time" while the process is going on, so neural network predictions will be available before the end of the process. Furthermore, once sufficient data for the initial teaching set are developed, the data base can be updated with new results to improve the net springback modeling capability under process variations.

ACKNOWLEDGEMENT

This work was funded in part by NSF grant #CMS-9622271.

REFERENCES

1. Sunseri, M., Cao, J., Karafillis, A. P., and Boyce, M. C., 1995, "Accomodation of Springback Error in Channel Forming Using Active Binder Force Control: Numerical Simulations and Results", J. Eng. Mat. And Techn., pp. 426-435
2. Karafillis, A. P., and Boyce, M. C., 1992, "Tooling Design in Sheet Metal Forming Using Springback Calculations", Int. J. Mech. Sci., 34, 113
3. Karafillis, A. P., and Boyce, M. C., 1996, "Tooling and Binder Design for Sheet Metal Forming Compensating Springback Error", Int. Jnl. Machine Tools and Manufacture, 36, 503
4. Ayres, R.A. 1984, "SHAPESET: a process to reduce sidewall curl springback in high-strength steels rails", J. Appl. Metalworking, 3, 127.
5. Rosenblatt, R., 1959, "Principles of Neurodynamics", New York, Spartan Books
6. Widroff, B. and Hoff, M. E., 1960, "Adaptive Switching Circuits", 1960 IRE WESCON Conv. Record, Part 4, pp. 96-104
7. Nguyen, D. and Widrow, B., 1989, " The truck Backer-upper: An Example of Self-learning in Neural Networks," Proc. Intl. Joint Conf. on Neural Networks", Vol2, pp. 357-363, Wash., DC.
8. Sejnowski, T. J. and Rosenberg, C. R., 1986, "Nettalk: a Parallel Network that Learns to Read Aloud," Tech. Rep. JHU/EECS-86/01, John Hopkins University
9. Bounds, D. G., Lloyd, P. J., Matthew, B. and Waddel, G., 1988, "A Multilayer Perceptron Network for the Diagnosis of Low Back Pain,"' Proc. 2d IEEE Intl. Conf. on Neural Networks, Vol. 2, pp. 481-489, San Diego, CA.
10. Bradshaw, G., Fozzard, R., and Ceci, L., 1989, "a Connectionist Expert System that Actually Works," in *Advances in Neural Network Information Processing Systems I*, Touretzky D. S., Ed. San Mateo, CA,: Morgan Kaufmann, pp. 248-255.
11. Elkins, K. L., 1994, "On-Line Angle Control for Small Radius Air Bending," Carnegie Mellon University, UMI Dissertation Services, Ph.D. Thesis, pp. 19-25, 90-95.
12. Yang M., Shima, S. and Watanabe, T., 1992, "Development of Control System Using Neural Network Combined with Deformation Model for an Intelligent V-Bending Process of Sheet Metals," Proc. Japan/USA Symposium on Flexible Automation, ASME, Vol. 2, pp. 1485-1490.
13. Forcellese, A., Gabrielli F. and Ruffini, R; 1997, "Springback Control in a Air Bending Process by Neural Network," Submitted for Proc. III Convegno AITEM.
14. Rumelhart, D.E. and Mc Clelland, J.L.; 1986, "Learning Internal Representation by Error Propagation," Parallel Distributed Processing, Vol. 1, Ch. 8, Eds., Cambridge, MA, MIT Press.
15. Widrow, B. and Lher, M.A.; 1990, "30 Years of Adaptive Neural Networks: Perceptron, Madaline and Backpropagation," Proc. of the IEEE, Vol. 78, N°9.
16. Stinchombe, M. and White, H.; 1989, "Universal Approximation using Feedforward Networks with Non-Sigmoid Hidden Layer Activation Functions," Proc. Int. Joint Conf. on Neural Networks, Vol. 1, Washington, DC: 613-617.
17. Cybenko, G.; 1988, "Continuous Valued Neural Networks With Two Hidden Layers Are Sufficient," Technical Report, Dep. of Computer Science, Tufts University.
18. Graf, A. and Hosford, W., 1993, Plane-strain Tension Test of AL 2008-T4 Sheets," Proc. SAE Congress Symposium on Sheet Forming, Detroit
19. Jalkh, P., Cao, J., Hardt, D., and Boyce, M. C., 1993, "Optimal forming of Aluminium 2008-T4 Conical Cups Using Force Trajectory Control," Proc. SAE Congress Symposium on Sheet Forming, Detroit, 101.
20. Stelson, K. A.; 1983, "Real Time Identification of Workpiece Material Characteristic from Measurements During Brakeforming," ASME J. of Engineering for Industry, Vol. 105, pp. 45-53.
21. [21] Stelson, K. A.; 1986, "An Adaptive Pressbrake Control for Strain Hardening Materials," ASME J. of Engineering for Industry, 108, pp. 127-132.
22. [22] Stelson K. A., Peterson, T. Y., 1989, "The Area-Coarea Method for the Estimation of Power-Law Constitutive Parameters," ASME J. of Engineering for Industry, Vol. 111, pp. 295-297.